Low Chirp EMLs Fabricated By Combining SAG and Double Stack Active Layer Techniques

Volume 10, Number 2, April 2018

Qiufang Deng
Hongliang Zhu
Xiao Xie
Lu Guo
Siwei Sun
Song Liang
Wei Wang

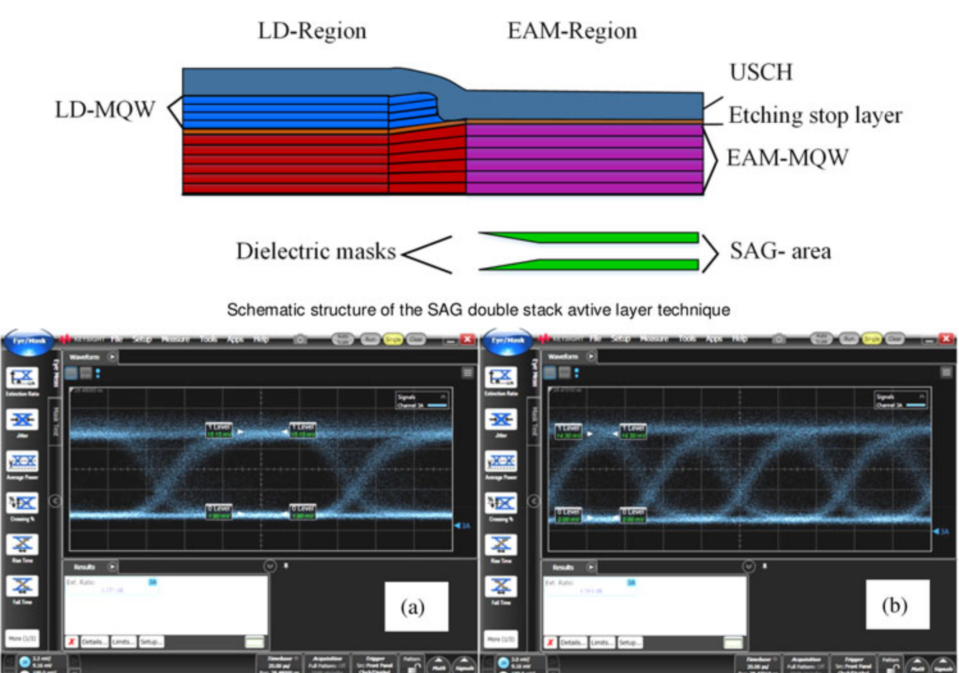

DOI: 10.1109/JPHOT.2018.2812837
1943-0655 © 2018 IEEE

Low Chirp EMLs Fabricated By Combining SAG and Double Stack Active Layer Techniques

Qiufang Deng[1,2,3] **Hongliang Zhu,**[1,2,3] **Xiao Xie,**[1,2,3] **Lu Guo**[1,2,3]
Siwei Sun[1,2,3] **Song Liang**[1,2,3] **and Wei Wang**[1,2,3]

[1]Key Laboratory of Semiconductor Materials Science, Institute of Semiconductors, Chinese Academy of Sciences, Beijing 100083, China
[2]College of Materials of Science and Opto-Electronic Technology, University of Chinese Academy of Sciences, Beijing 100049, China
[3]Beijing Key Laboratory of Low Dimensional Semiconductor Materials and Devices, Beijing 100083, China

DOI:10.1109/JPHOT.2018.2812837
1943-0655 © 2018 IEEE. Translations and content mining are permitted for academic research only. Personal use is also permitted, but republication/redistribution requires IEEE permission. See http://www.ieee.org/publications_standards/publications/rights/index.html for more information.

Manuscript received January 9, 2018; revised March 1, 2018; accepted March 2, 2018. Date of publication March 7, 2018; date of current version March 26, 2018. This work was supported in part by the National Natural Science Foundation of China under Grant 61320106013, Grant 61474112, Grant 61635010, Grant 61574137, Grant 61321063, and Grant 61274071; and in part by the National Key Research and Development Program of China under Grant 2016YFB0402301. Corresponding author: Song Liang (e-mail: liangsong@semi.ac.cn).

Abstract: We present electroabsorption modulators integrated with distributed feedback lasers (EMLs) fabricated by a simple method, which combines the advantages of the selective area growth and double stack active layer techniques. The obtained EML device has a threshold current as low as 16 mA and optical power of larger than 10 mW at 85 mA laser current. Quite low chirp parameter of the fabricated EMLs is obtained. Negative chirp parameters can be obtained at only about 0.5 V reverse bias voltage. Open eye diagrams are demonstrated from the EML at both 10 and 20 Gb/s modulations with the driving voltage of only 0.65 V while securing high dynamic extinction ratio. The exhibited performance makes our device a very promising candidate as a simple light source in long distance and cost sensitive applications.

Index Terms: Electroabsorption-modulated DFB lasers, low chirp parameters, low driving voltage, selective area growth, double stack active layer.

1. Introduction

Due to the explosive increase of data traffic, low-cost large-capacity optical communication systems are urgently needed. Lasers based on different material systems [1]–[12] are key components in these systems. Electroabsorption modulator (EAM) integrated distributed feedback (DFB) lasers (EMLs) have been deemed as an appropriate candidate for such optical communication systems especially in the long haul case due to their advantages of low chirp, compactness, low cost, low driving voltage and high stability [3]–[12]. Currently, commercially available EMLs are usually fabricated by either the butt-joint technique [5], [9], [10] or the selective area growth (SAG) technique [4], [11], [12]. In the butt-joint technique [9], [10], the EAM multi-quantum well (MQW) material is butt-jointed with the laser material in a separated epitaxy run, so the EAM material can be optimized separately. However, the butt-joint growth conditions needs to be optimized carefully

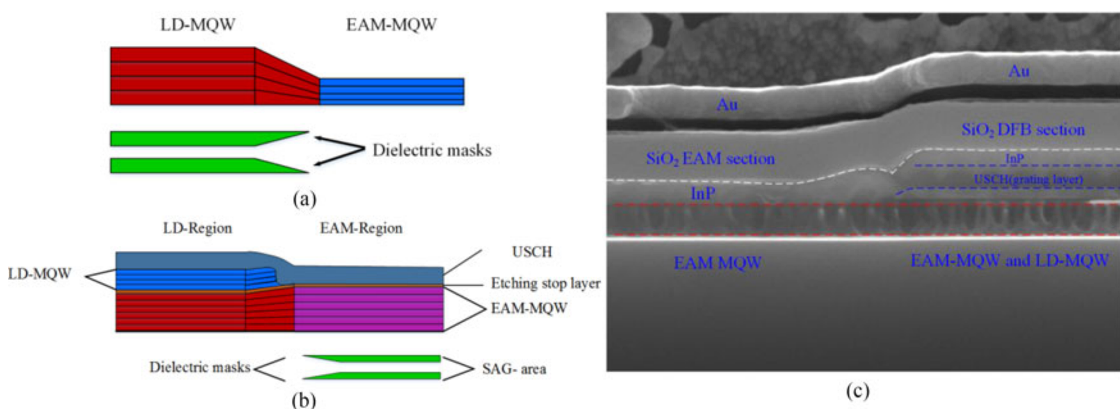

Fig. 1. Schematic structures of conventional SAG technique (a) and SAG double stack layer technique (b) and the SEM image of the grown material.

to obtain a high quality interface between the laser and butt-jointed materials. In conventional SAG processes [11]–[14], both the laser and modulator materials can be obtained in a single epitaxy run, simplifying the fabrication process significantly. However, the parameters of the MQW materials for high performance EAMs and laser diodes (LDs) cannot be optimized at the same time. For fabricating high quality EMLs, we developed a process which combines the advantages of the SAG technique and the double stack active layer technique. As shown in Fig. 1, pairs of dielectric masks are formed in the EAM areas in the process, which is contrary to the usual SAG method [12]. Then, the EAM MQWs and the LD MQWs are grown successively in a single metal–organic chemical vapor deposition (MOCVD) growth on the patterned substrate. After the growth, the LD MQWs in the EAM areas are selectively etched off by the usual photolithography and wet etching, leaving only the EAM MQWs in the EAM section. Similar to the usual SAG technique, only one epitaxy run is needed to get both the modulator and laser MQWs. What makes it different is that, the successive growth of the EAM MQWs and LD MQWs makes it easy to optimize the two kinds of MQW material separately, which is similar to the double stack active layer technique. Because the SAG masks are placed in the EAM section, the bandgap wavelength of the bottom MQWs in the laser section can be set as being over 100 nm shorter than the upper laser MQWs, reducing the effects of the bottom MQWs on the laser performance greatly.

In this paper, we present low chirp operation of EMLs fabricated by the process which combines the SAG and double stack active layer techniques. Negative chirp parameters can be obtained at only about 0.5 V reverse bias. Open eye diagrams are demonstrated from the EML at both 10 and 20 Gb/s modulations.

2. Device Design and Fabrication

MOCVD is used for the growth of the EML material. Details of the material growth and device fabrication procedures can be found in reference [15]. The schematic structures of the fabricated device and the scanning electron microscope (SEM) image are shown in Fig. 1. The photoluminescence wavelength of the laser MQWs is 1.55 μm. The laser MQWs consist of 6 compressively strained InGaAsP wells ($+1.1 \times 10^{-2}$) and 7 tensile strained InGaAsP barriers (-3×10^{-3}, $\lambda_{PL} = 1.2\,\mu$m). The EAM MQWs also have a strain compensated structure. By optimizing the parameters of the quantum wells and barriers, the height of the valance band offset is reduced to obtain a low chirp parameter of modulator [16], without damaging the extinction properties of the EAM notably. The modulator MQWs consist of 10 compressively strained InGaAsP wells ($+1.1 \times 10^{-2}$) and 11 tensile strained InGaAsP barriers (-3×10^{-3}, $\lambda_{PL} = 1.2\,\mu$m) and have a 1.50 μm PL wavelength in the EAM section. Before the material growth, SiO_2 SAG mask stripes are first formed on the

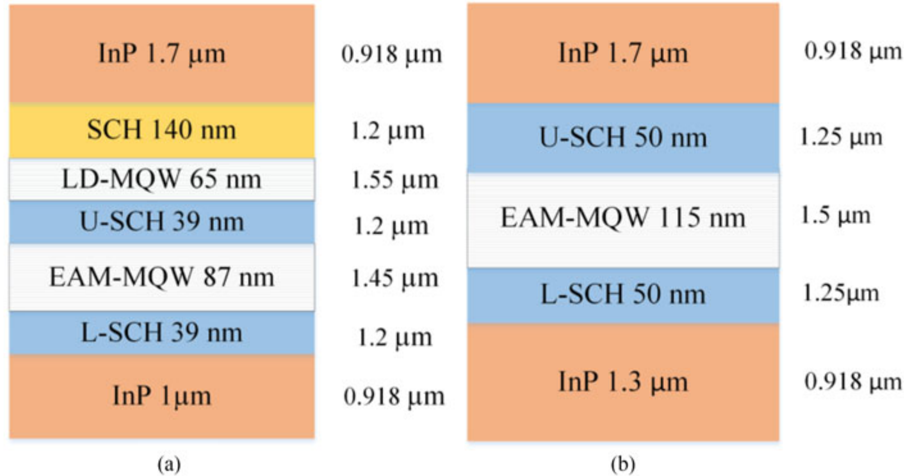

Fig. 2. The schematic material structures of DFB section (a) and EAM section (b).

substrate in the EAM areas of the wafer. During the following MOCVD growth, no material is nucleated and grown on the masks and material deposition happens only in the area where there is no SiO_2 mask. The growth rate of the MQWs between the masks, which is used as modulator material, is enhanced and the composition of the material is also different from that on bare substrates. As a result, the emission wavelength of the modulator MQWs in the DFB areas is shorter than that of the MQWs in the modulator region, where there are no masks. The geometry of mask patterns including mask width and separation can be used to tune the above wavelength difference, which is 50 nm in our device. Thus the EAM MQW in the laser section is 1.45 μm, which is about 100 nm shorter than that of the laser MQWs, helping to lower their effects on the laser performance. The schematic material structures of the LD section and EAM section are shown in fig. 2. Grating with a period of 242.5 nm is formed in the 140 nm InGaAsP layer above the laser MQWs in the laser section as shown in Fig. 1. (c) by holographic exposing and dry etching. The coupling coefficient is 58.9/cm.

The length of the total device is 500 μm, consisting of a 300-um laser section and a 150-μm EAM. A 50-μm isolation trench is inserted between the two parts to avoid electrical crosstalk. A 3-μm ridge waveguide is adopted for both the DFB laser and the EAM. Before testing, dielectric high reflection ($>$70%) coating and anti-reflection ($<$1%) coating layers are deposited on the laser facet and modulator output facet, respectively.

3. Device Measurements and Discussions

The device is sintered on an AlN heat sink and the temperature is controlled at 20 °C by a thermoelectric cooler (TEC). Fig. 3(a) shows the typical light output power from the EAM facet as a function of injection current (L-I) of DFB laser when the EAM is zero biased. As can be seen, the threshold current of the device is 16 mA. And the output power is larger than 10 mW at an injection current of 85 mA. A typical optical spectrum of the fabricated EML is shown in Fig. 3(b). When the injection current of the laser is set at 64 mA, the wavelength of the light is 1552.28 nm. The side band suppression ratio (SMSR) of the spectrum is larger than 53 dB. As shown in the figure, there are multiple peaks on the sides of the emission, which might be related to the interface between the DFB laser and EAM and has also been observed in an EML fabricated by butt-joint technique [17]. Light transmission in our EML device is simulated with beam propagation method (BPM). It is shown that the transmission loss related to the interface between the EAM and DFB laser is less than 3%. The light reflection from the interface should then be smaller than 3%, because part of

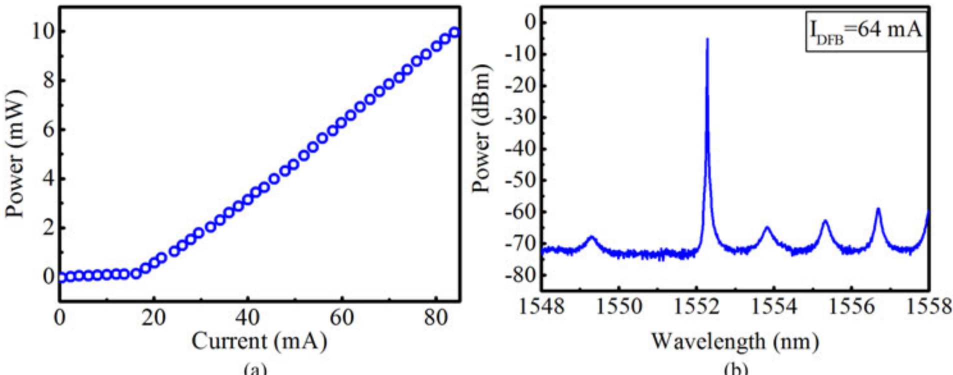

Fig. 3. (a) The power vs. injection current characteristics of the device, (b) a typical optical spectrum of the EML.

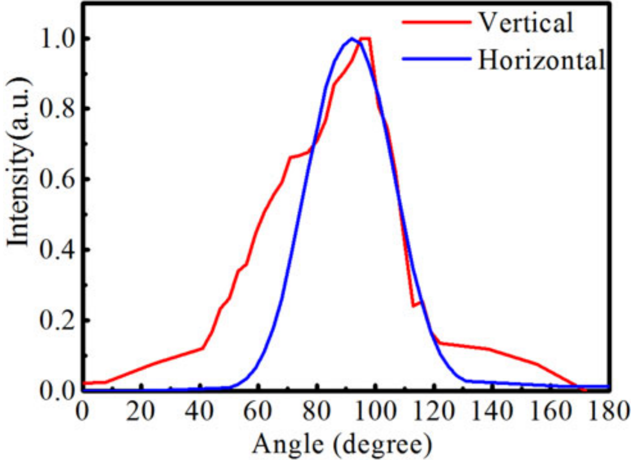

Fig. 4. Far field distribution of the EML.

the light loss is deflected out of the waveguide. The far field distribution measured from the EAM facet is shown in Fig. 4. The divergence angles (full width at half maximum (FWHM)) are 34.2° and 47.3° in the horizontal and vertical directions, respectively.

Fig. 5(a) shows the static extinction ratio of the device as a function of the EAM reversed bias voltage when the current of the DFB laser is set at 64.5 mA. As can be seen, over 30 dB static extinction ratio can be obtained at −5 V EAM bias. A 50 GHz network analyzer is used for measuring the small signal frequency response of the modulator. The obtained E/O response at different EAM bias voltage is shown in Fig. 5(b). The small signal 3 dB bandwidth increases from 6 to 10 GHz when the bias voltage is increased gradually from 0.4 to 2 V. As can be seen from the figure, there is response decay at low modulation frequencies for some bias conditions, whose effects on the device performance are not clear by now. Fortunately, the decay is shown only when the bias voltage is larger than 0.8 V. Clearly opened eyes can be observed when the biased voltage is 0.65 V and it will be shown below.

The chirp parameter of the modulator is obtained by the fiber peak method [18]. The EML device is modulated by a 50 GHz network analyzer. The modulated optical signal shows a phase modulation due to the chirp of the modulator. After transmission in a 25-km standard single mode fiber (SMF), there are some fading points in the small signal response curve as shown in Fig. 6(a). Chirp parameter can be extracted by counting the frequencies and orders of resonances [18].

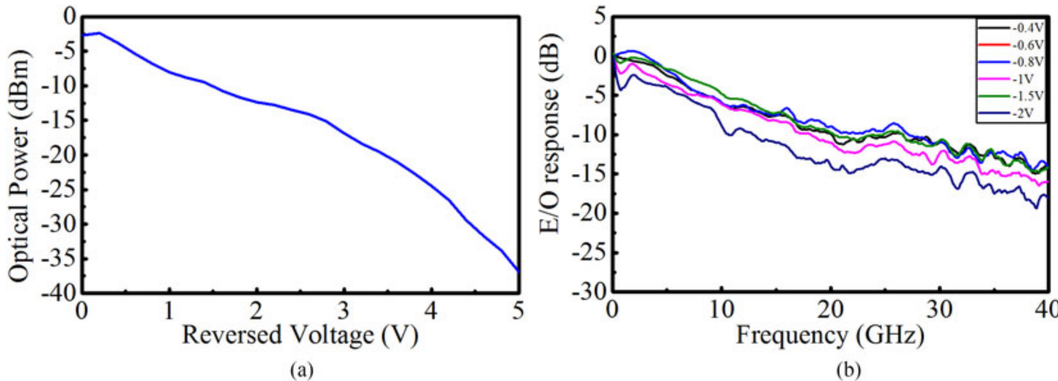

Fig. 5. (a) Fiber coupled output power vs. reverse bias of the EML device, (b) electro-optic small signal response of the fabricated EML under different bias voltages.

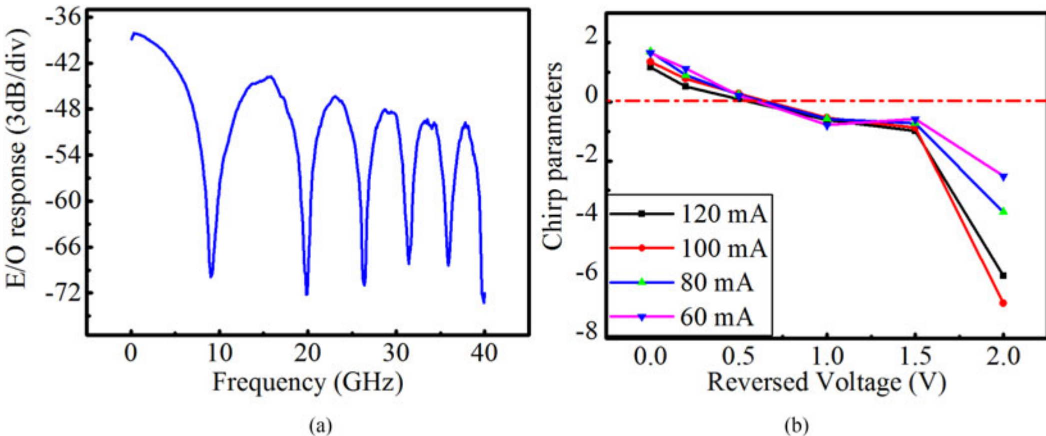

Fig. 6. (a) An example of the frequency response of the fabricated EML measured by fiber peak method (with 25 km standard single mode fiber), (b) measured reverse bias voltage dependence of the α parameter when the current of the DFB laser ranges from 60 mA to 120 mA.

Fig. 6(b) shows the reverse bias voltage dependence of the chirp parameter at four different DFB laser currents. It can be seen that negative chirp parameters can be obtained when the reverse voltage is larger than 0.5 V at all cases. This voltage is lower than that reported in previous papers [4], [5], [7], [11], [19], showing superiority of the proposed technique because a lower bias voltage applied to EAM means a larger output power since the insertion loss in EAM is reduced. Therefore, the low chirp parameter and larger output power both guarantee a long transmission distance. The chirp parameter decreases more rapidly as the laser wavelength approches the absorption edge of the EAM [16], which is redshifted as the reverse bias is increased. This results in the obvious drop of the chirp parameter after 1.5 V reverse bias as shown in Fig. 6(b).

The eye diagrams of the chip are measured when the modulator is modulated with non-return to zero (NRZ), $2^{31} - 1$ pseudorandom bit stream (PRBS) signal at 10 and 20 Gb/s. The modulator reverse bias voltage is 0.65 V and the laser current is 64 mA. The RF voltage swing is 2.7 V_{pp}. The modulated light power from the chip is about 2 mW. The 10 Gb/s eye diagrams in back to back (BTB) configuration and after 25-km transmission on SMF are shown in Fig. 7(a) and (b), respectively. Clearly opened eyes can be obtained under both the conditions. The dynamic extinction ratios (DER) are larger than 9 dB for both the BTB and 25-km transmission conditions. Fig. 7(c) and (d) show the eye diagrams at 20 Gb/s. The DERs are 8.6 dB and 5.6 dB for the BTB and 25-km transmission conditions, respectively.

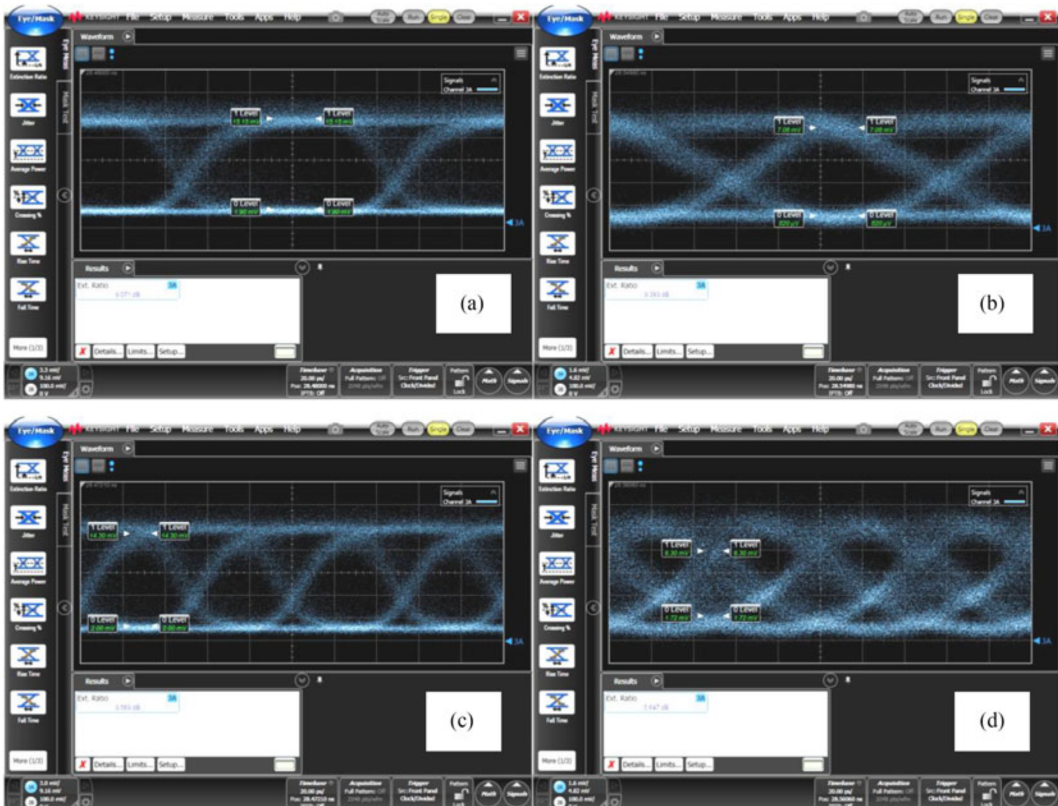

Fig. 7. Large signal eye diagrams (a) 10 Gb/s back-to-back configuration, (b) 10 Gb/s after 25 km transmission through SMF, (c) 20 Gb/s back-to-back configuration, (d) 20 Gb/s after 25 km transmission through SMF.

We compare the performance between the EML in this paper and an EML we have fabricated with the butt-joint technique as shown in [20]. The active MQWs of the DFB section of the butt-joint EML have all the same parameters as the device in the present manuscript, but having symmetric separate confinement heterostructure (SCH) layers. Except 6 wells, the MQWs of the EAM of the EML also have the same parameters as the modulator MQWs in the present device. Besides, both the EMLs have the same ridge width and section lengths. It is shown that the presence of the EAM MQWs below the active MQWs leads to some degradation of the device performance. The threshold current is increased from 13 mA to 16 mA and the output power is decreased from 11 mW to 9 mW at 80 mA DFB current.

4. Conclusion

EMLs are fabricated by a novel method which combines the advantages of the selective area growth (SAG) and double stack active layer techniques. The successive growth of the EAM MQWs and laser MQWs makes it easy to optimize the two kinds of MQW material separately. Because the SAG masks are placed in the EAM section, the bandgap wavelength of the bottom MQWs in the laser section can be over 100 nm shorter than the upper laser MQWs, reducing the effects of the bottom MQWs on the laser performance greatly, which is difficult to be realized in conventional double stack active layer techniques. Negative chirp operation of the obtained EMLs can be obtained at only about 0.5 V reverse bias. And open eye diagrams are demonstrated from the EML at both 10 and 20 Gb/s modulations with a driving voltage of only 0.65 V. The device proves to be a promising candidate for cost effective and energy-efficient transmitters used in long distance transmission.

Acknowledgment

The authors would like to thank the International Lab of Photonic Integrated Circuits for help and support.

References

[1] K. Xu, “Integrated silicon directly modulated light source using p-well in standard CMOS technology,” *IEEE Sensors J.*, vol. 16, no. 16, pp. 6184–6191, Aug. 2016.
[2] S. Chen *et al.*, “Electrically pumped continuous-wave III–V quantum dot lasers on silicon,” *Nature Photon.*, vol. 10, no. 5, pp. 307–311, 2016.
[3] H. Fukano, T. Yamanaka, M. Tamura, and Y. Kondo, “Very-low-driving-voltage electroabsorption modulators operating at 40 Gb/s,” *J. Light. Technol.*, vol. 24, no. 5, pp. 2219–2224, May 2006.
[4] Yuanbing Cheng *et al.*, “40-Gb/s low chirp electroabsorption modulator integrated with DFB laser,” *IEEE Photon. Technol. Lett.*, vol. 21, no. 6, pp. 356–358, Mar. 2009.
[5] H. Fukano *et al.*, “Low chirp operation of 40 Gbit/s electroabsorption modulator integrated DFB laser module with low driving voltage,” *IEEE J. Sel. Topics Quantum Electron.*, vol. 13, no. 5, pp. 1129–1134, Sep./Oct. 2007.
[6] T. Fujisawa, Y. Ueda, H. Sanjoh, S. Kanazawa, T. Ito, and W. Kobayashi, “Advantages of EADFB laser for 25 Gbaud/s 4-PAM (50 Gbit/s) modulation and 10 km single-mode fibre transmission,” *Electron. Lett.*, vol. 50, no. 9, pp. 683–685, Apr. 2014.
[7] J. Kreissl, C. Bornholdt, T. Gaertner, L. Moerl, G. Przyrembel, and W. Rehbein, “Flip-chip compatible electroabsorption modulator for up to 40 Gb/s, integrated with 1.55 μm DFB laser and spot-size expander,” *IEEE J. Quantum Electron.*, vol. 47, no. 7, pp. 1036–1042, Jul. 2011.
[8] S. Makino *et al.*, “High-speed EA-DFB laser for 40-G and 100-Gbps,” *IEICE Trans. Electron.*, vol. E92–C, no. 7, pp. 937–941, 2009.
[9] W. Kobayashi *et al.*, “Design and fabrication of 10-/40-Gb/s, uncooled electroabsorption modulator integrated DFB laser with butt-joint structure,” *J. Light. Technol.*, vol. 28, no. 1, pp. 164–171, Jan. 2010.
[10] W. Kobayashi *et al.*, “Novel approach for chirp and output power compensation applied to a 40-Gbit/s EADFB laser integrated with a short SOA,” *Opt. Exp.*, vol. 23, no. 7, pp. 9533–9542, Apr. 2015.
[11] Y. Cheng, Q. J. Wang, and J. Pan, “1.55 μm high speed low chirp electroabsorption modulated laser arrays based on SAG scheme,” *Opt. Exp.*, vol. 22, no. 25, pp. 31286–31292, Dec. 2014.
[12] J. Xu, S. Liang, Z. Zhang, J. An, H. Zhu, and W. Wang, “EML array fabricated by SAG technique monolithically integrated with a buried ridge AWG multiplexer,” *Opt. Laser Technol.*, vol. 91, no. November 2016, pp. 46–50, Jun. 2017.
[13] C. Zhang, S. Liang, H. Zhu, L. Han, and W. Wang, “Multichannel DFB laser arrays fabricated by upper SCH Layer SAG technique,” *IEEE J. Quantum Electron.*, vol. 50, no. 2, pp. 92–97, Feb. 2014.
[14] C. Zhang *et al.*, “Multi-channel DFB laser arrays fabricated by SAG technology,” *Opt. Commun.*, vol. 300, pp. 230–235, Jul. 2013.
[15] H. Zhu, S. Liang, L. Zhao, D. Kong, N. Zhu, and W. Wang, “A selective area growth double stack active layer electroabsorption modulator integrated with a distributed feedback laser,” *Chin. Sci. Bull.*, vol. 54, no. 20, pp. 3627–3632, Oct. 2009.
[16] M. Matsuda, K. Morito, K. Yamaji, T. Fujii, and Y. Kotaki, “A novel method for designing chirp characteristics in electroabsorption MQW optical modulators,” *IEEE Photon. Technol. Lett.*, vol. 10, no. 3, pp. 364–366, Mar. 1998.
[17] T. Shindo *et al.*, “High modulated output power over 9.0 dBm with 1570-nm wavelength SOA assisted extended reach EADFB laser (AXEL),” *IEEE J. Sel. Topics Quantum Electron.*, vol. 23, no. 6, pp. 1–7, Nov. 2017.
[18] F. Devaux, Y. Sorel, and J. F. Kerdiles, “Simple measurement of fiber dispersion and of chirp parameter of intensity modulated light emitter,” *J. Light. Technol.*, vol. 11, no. 12, pp. 1937–1940, Dec. 1993.
[19] M. N. Ngo *et al.*, “ElectroAbsorption modulated laser integrated with a semiconductor optical amplifier for 100-km 10.3 Gb/s dispersion-penalty-free transmission,” *J. Light. Technol.*, vol. 31, no. 2, pp. 232–238, Jan. 2013.
[20] Y. Cheng *et al.*, “A novel butt-joint scheme for the preparation of electro-absorptive lasers,” *J. Phys. D, Appl. Phys.*, vol. 41, no. 3, Feb. 2008, Art. no. 035108.